A STUDY OF THE D WAVE IN THE K^+K^- SYSTEM OF THE REACTION $\pi^-p \to K^+K^-n$ AT 18 GeV

CERN-Cracow-Munich Collaboration

V. CHABAUD, J. DE GROOT, B. HYAMS AND T. PAPADOPOULOU[+]

CERN, Geneva, Switzerland

B. NICZYPORUK, M. RÓŻAŃSKA AND K. RYBICKI

Institute of Nuclear Physics, Kawiory 26a, 30-055 Cracow, Poland

H. BECKER[++], G. BLANAR, W. BLUM, H. DIETL, J. GALLIVAN[+++], B. GOTTSCHALK[*], E. LORENZ, G. LÜTJENS, G. LUTZ, W. MÄNNER, D. NOTZ[**], R. RICHTER, U. STIERLIN AND B. STRINGFELLOW[***]

Max Planck Institute, Munich, West Germany

(Received December 11, 1980)

The reaction $\pi^-p \to K^+K^-n$ has been studied on a hydrogen target (27000 events) at 18.4 GeV and on a butanol target (54000 events) at 17.2 GeV. In this paper we study the D wave fitting the superposition of $f(1270)+A_2(1310)+f'(1515)$ resonances to the t_0^4 moment. This fit gives very high $\chi^2/ND = 60/22$ for each sample if the parameters of f'(1515) are fixed at their table values. If these parameters are left free we obtain $m_{f'} = (1503^{+6}_{-7})$ MeV, $\Gamma_{f'} = (144^{+19}_{-17})$ MeV, and $BR(f' \to \pi\pi/f' \to all) = (3.0 \pm 1.0)\%$. Fixing the parameters of f'(1515) to their table values we obtain a good fit after the introduction of a fourth tensor meson with $m = (1422 \pm 9)$ MeV and $\Gamma = (80 \pm 42)$ MeV. Such an object does not easily fit into the quark-antiquark scheme.

PACS numbers: 13.85.-t, 13.85.Hd

+ Now at the National Technical University, Athens, Greece.
++ Now at the Technische Fachhochschule, Saarbrücken, West Germany.
+++ Now at the British National Oil Corporation, Glasgow, United Kingdom.
* Now at the Northeastern University, Boston, Massachusetts, USA.
** Now at DESY, Hamburg, West Germany.
*** Now at the Nuclear Research Centre, Strasbourg, France.

1. Introduction

The quantum numbers of a system decaying into K^+K^-, characterized by spin J and isospin I, are $P = C = (-1)^J$; thus $J^{PC} = 0^{++}, 1^{--}, 2^{++}, \ldots$ and $G = (-1)^{J+I}$. In general, the reaction

$$\pi^- p \rightarrow K^+K^- n \quad (1)$$

is observed to be dominated by one pion exchange (OPE). This production mechanism leads to a K^+K^- system with even G-parity, i.e. to the following resonances: S*(980), ε(1300), f(1270), f′(1515), g(1690), h(2040) etc. Another production mechanism is needed for $\phi(1020)$ and $A_2(1310)$ resonances. The least known of the tensor mesons is the f′(1515) resonance, believed to consist of strange quarks, thus favouring the decay into $K\bar{K}$. In spite of a considerable experimental effort, the parameters of the f′(1515) are still rather controversial. This is generally due to a small production cross-section, to an Okubo-Zweig--Iizuka (OZI) rule ban, suppressing its coupling to the $\pi^+\pi^-$ channel, and to interference with the f(1270) and possibly the $A_2(1310)$ resonances.

In this paper we present the study of the D-wave K^+K^- resonances. This study is based on the results of two experiments on reaction (1) at ~ 18 GeV[1]. They were performed at the CERN Proton Synchrotron with the CERN-Munich Spectrometer, designed to study peripheral quasi two-body processes off hydrogen and a polarized target.

A partial wave analysis of the K^+K^- system based on the results of these experiments is described in Ref. [1]. It is a model-independent and energy-independent analysis, yielding intensities of partial waves. These intensities can in turn be fitted by Breit-Wigner formulae. In this paper, a different approach is followed. We fit a superposition of Breit-Wigner formulae directly to the moments. We use the moments of the hydrogen experiment as well as the polarization independent moments obtained with the butanol target. This procedure leads to smaller errors of parameters, but is necessarily based on some assumptions, discussed in Section 4, as we do not use the polarization data in this analysis.

This paper is organized as follows. In Section 2, the selection and processing of K^+K^- events are discussed. The moments of the angular distribution are presented in Section 3. Section 4 is devoted to a multi-resonance fit to the t_0^4 moments between 1.025 and 1.70 GeV mass, (t_0^4 is the unnormalized $L = 4$, $M = 0$ moment of the K^+K^- decay angular distribution). The results for the D-wave resonances are extensively discussed in Section 5. In Section 6, a fit including a new D-wave state is described.

2. The data

The data for this analysis come from two experiments using different targets:

(I) An experiment with a liquid hydrogen target at 18.4 GeV incident momentum,

(II) An experiment using a polarized target (butanol C_4H_9OH) at 17.2 GeV incident momentum.

---

[1] Hereafter c is omitted in all dimensions.

The reaction (1) was part of an experimental programme to study quasi-two-body reactions off hydrogen and off a polarized target, therefore the general experimental procedure and the detectors have been already extensively described in Ref. [2] for the hydrogen target arrangement and in Ref. [3] for the experiments off butanol. Here we will only describe the data selection procedure relevant to reaction (1).

Fig. 1 shows the basic layout of the spectrometer for the hydrogen target arrangement. Incident pions interact in a 50 cm hydrogen target. Charged forward-going 2-prong events ($\pi^+\pi^-$, K^+K^-, $p\bar{p}$-pairs) are selected by a 32 element scintillation counter hodoscope S8.

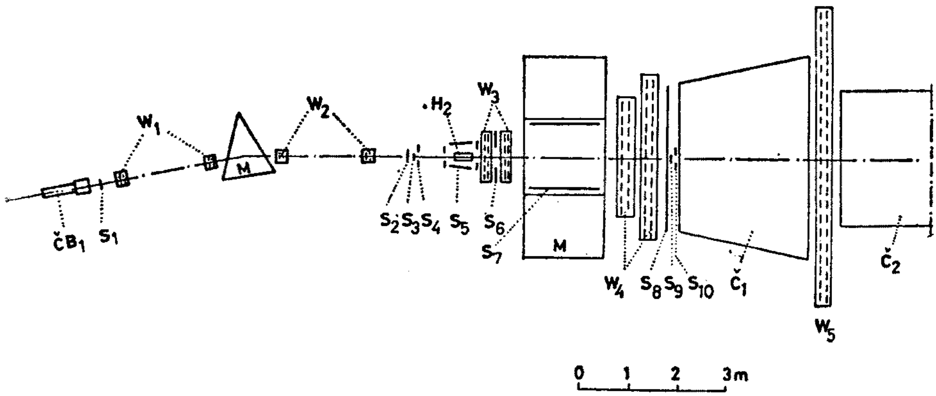

Fig. 1. Schematic view of the apparatus

The directions of the secondary tracks are measured in a spark chamber set W3 and their momenta by the spectrometer formed by a wide gap magnet M ($150 \times 50\ cm^2$ window, 2 Tm bending power) and the 2 spark chamber sets W3 and W4. Identification of the secondaries was performed by two Čerenkov counters Č1 and Č2.

In the trigger we required that no charged particle or π^0 left the target under wide angles by demanding no signal in the lead sandwich counters S5 around the target or counters S6 around the magnet window. Further anticoincidence counters S7 lined the magnet pole faces and coils. The spark chamber set W5 behind Č1 helped to purify the $K\bar{K}$-pair (as well as the $p\bar{p}$-pair) sample by demanding that the faster secondary track passed the Čerenkov counter Č1 without secondary interaction or decay.

In the polarized target experiment the hydrogen target was exchanged for a polarized butanol target.

Table I summarizes the essential run parameters. For the two data sets we used slightly different fillings of the Cerenkov counter Č1, taking the different beam momenta into account (see Table I). A different trigger mode was also used. For data set I, the Čerenkov counter Č1 was included in the trigger, vetoing π-pair production, while for data set II, π^-, K^-, $p\bar{p}$-pairs were recorded together. The separation of the different channels was performed offline. Fig. 2 shows the efficiency curves for Č1 (pions) and Č2 (Kaons). It should be mentioned that we could identify only the faster secondary particle, thus making use of strangeness or baryon number conservation.

TABLE I

	SET I	SET II	COMMENTS
target	hydrogen	butanol	
polarization	—	68 %	
incident momentum	18.4 GeV	17.2 GeV	
number of recorded triggers	3.3×10^6	2×10^7	π-pairs suppressed in set I
Number of good K^+K^-n events	27000	54000	
$\pi\pi n$ background	1 %	<1 %	
$KKn\pi^0$ background	2 %	2 %	
$p\bar{p}n$ background	1 %	~1 %	
$K^*\Lambda$ background	0.4 %	0.4 %	π of K^* decay below 5.5 GeV
invariant mass resolution	5 MeV	5.5 MeV	at 1.3 GeV KK-mass
π threshold for Č1	5.3 GeV	5.0 GeV	N_2-CO_2 filling
K threshold for Č1	18.6 GeV	17.5 GeV	
p threshold for Č1	35.5 GeV	33.2 GeV	
π threshold for Č2	2.3 GeV	2.3 GeV	Neopentane filling,
K threshold for Č2	8.3 GeV	8.3 GeV	pulse height discrimination
p threshold for Č2	15.7 GeV	15.8 GeV	of p, K above 15.7 GeV
overall correction factor	$w = 1.30$	$w = 1.69$	
σ_{1event} in corrected sample in nb	0.13 ± 0.006	0.042 ± 0.002	

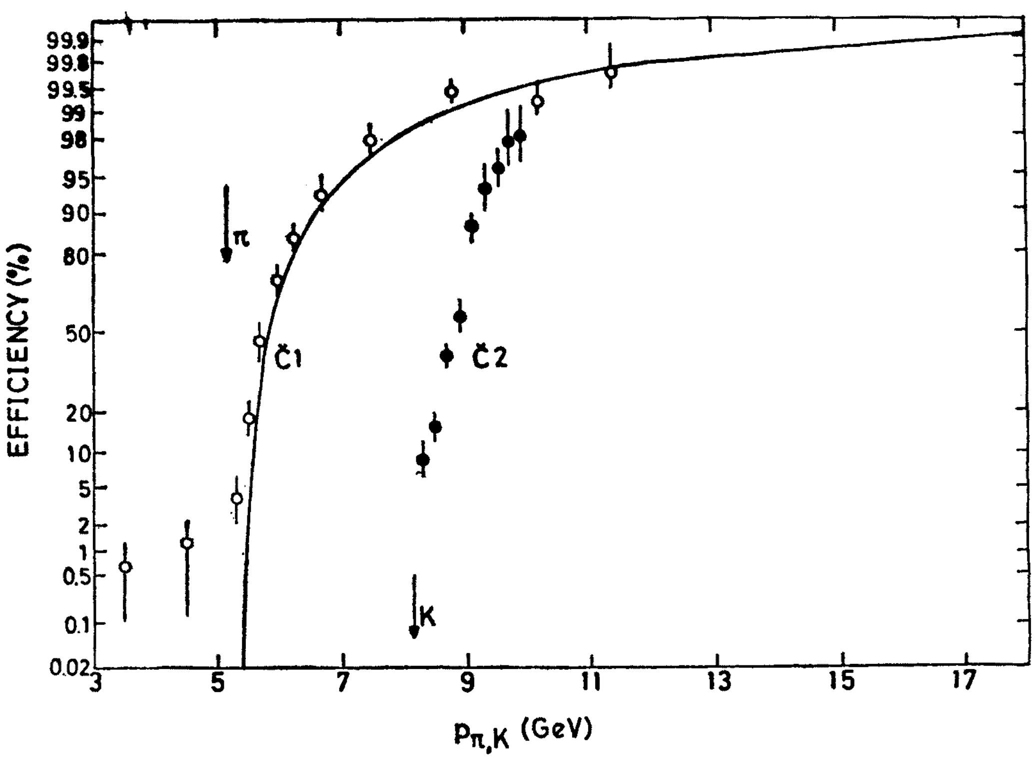

Fig. 2. The efficiency of the Čerenkov counters for pions (Č1) and kaons (Č2)

In these experiments the recoil neutron is not directly observed but identified from the missing mass after the event reconstruction. Fig. 3 shows the missing mass distribution for both data sets. Both sets show clear peaks around the neutron mass, while a certain

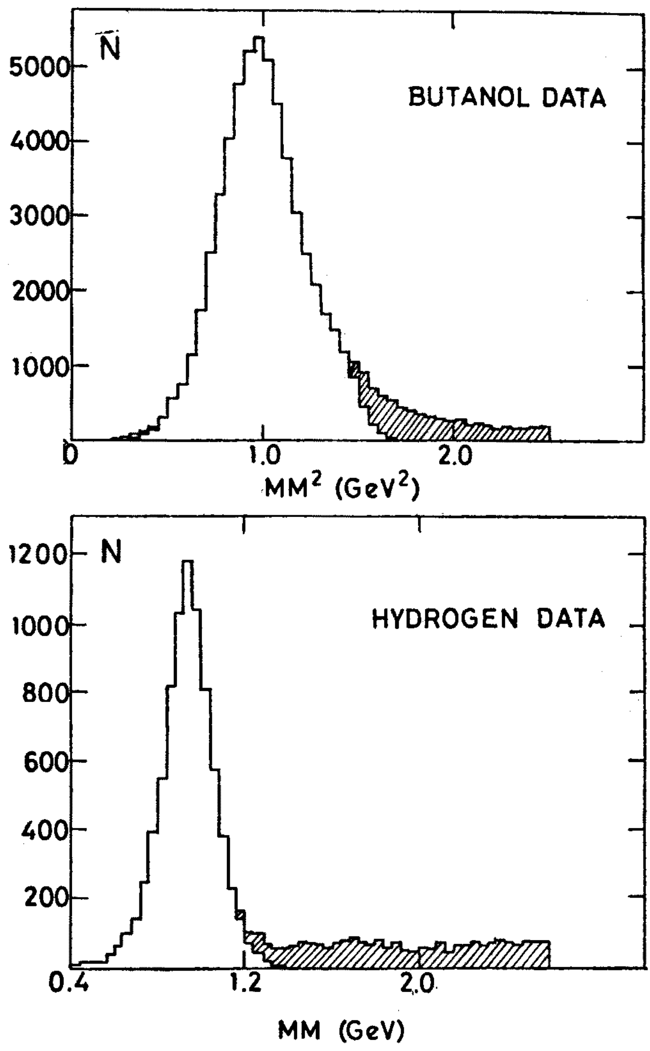

Fig. 3. Missing mass distribution for $\pi^- p \rightarrow K^+K^-$ MM: a) MM^2 for butanol data, b) MM for hydrogen data

broadening due to Fermi motion is observed in set II. After appropriate cuts we obtain fairly pure samples of K^+K^-n events with the background contributions listed in Table I. For data set II we do not distinguish between the production of K-pairs off free or bound protons.

The observed spectra were corrected for the acceptance losses caused by the geometry of our detector. For set I we randomly rotated the events around their beam direction and tested their acceptance. Small effects of the vertex distribution and incident particle direction were also taken into account. This correction procedure was possible because the apparatus allowed the observation of K-pairs up to 2.4 GeV mass and $|t|$ (= square of the four-momentum transfer from the incident proton to the final neutron) less than

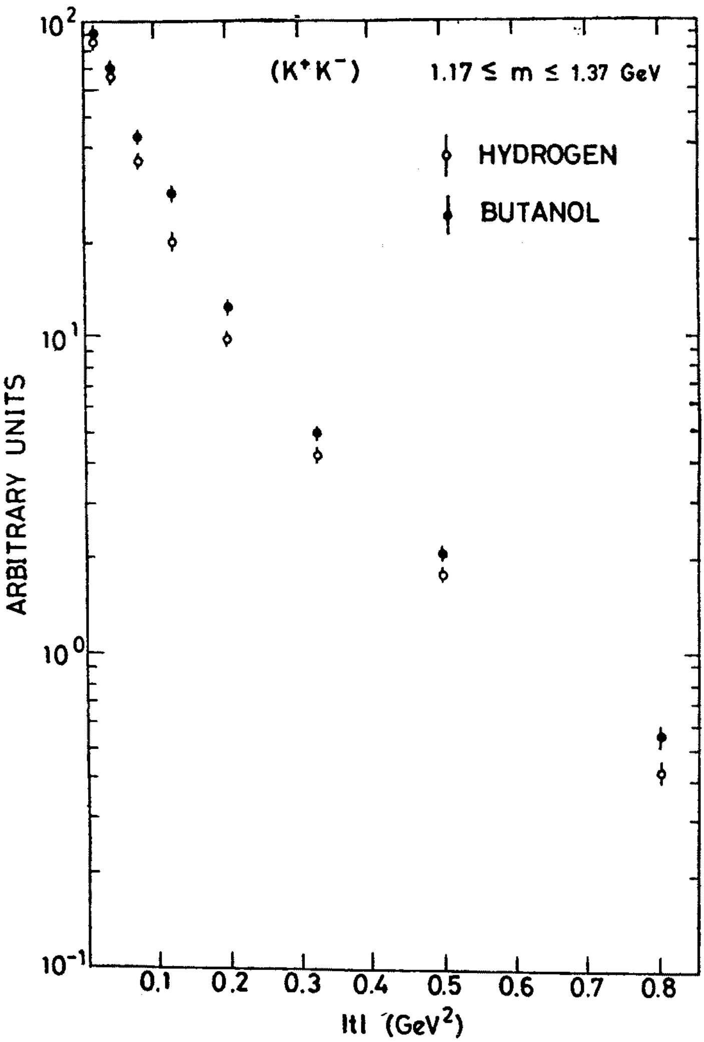

Fig. 4. t-dependence of the K^+K^- cross-section in the f region ($1.17 < m_{KK} < 1.37$ GeV) for hydrogen and butanol data)

$|t| < 1\ GeV^2$ over the full range of the decay angles in the $K\overline{K}$ centre of mass system. Details of the method are described in Ref. [2]. For set II this procedure is not applicable because of the polarization effects. Here the method of moments generalized for the polarized target experiment was used as described in Ref. [3]. The acceptance in the mass region between 1.1 ad 1.5 GeV was close to 80% for both target arrangements.

The individual events were further weighted for decay in flight losses, inefficiencies of the Čerenkov counters, secondary interactions inside the target and losses from δ-rays and recoil neutrons, detected by the anticoincidence system. Configuration independent

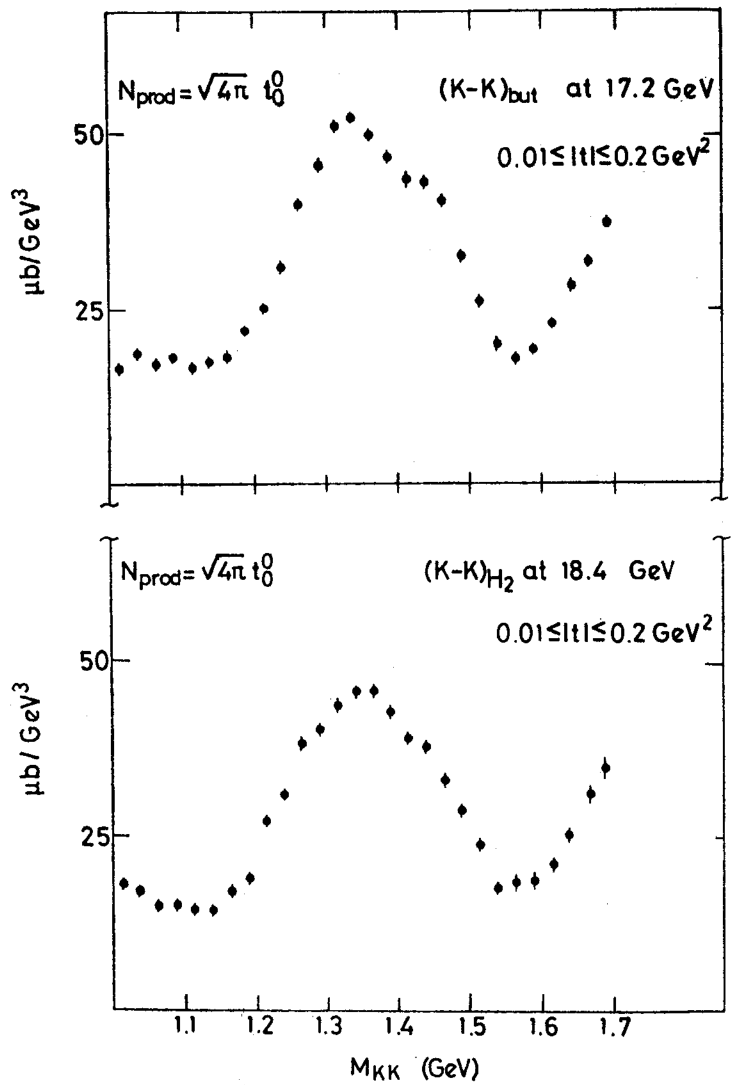

Fig. 5. K^+K^- invariant mass spectrum for $0.01 < |t| < 0.2$ GeV^2 for butanol and hydrogen data

losses (i.e. losses due to electronics inefficiency, extra beam tracks, secondary interactions in the setup, reconstruction losses, beam contamination, etc.) were applied to the number of incident pions for the cross-section calculation. The overall correction factors were

$w = 1.3$ for set I and $w = 1.69$ for set II respectively. The cross-sections per event are:

$$\sigma_{1\ \mathrm{event}} = (0.13 \pm 0.006)\ \mathrm{nb} \qquad \text{sample I},$$

$$\sigma_{1\ \mathrm{event}} = (0.042 \pm 0.002)\ \mathrm{nb} \qquad \text{sample II}.$$

As already mentioned, we were not able to distinguish the production of K-pairs off free and bound protons for data set II. About two thirds of our second sample corresponds to interactions with bound protons. Since we cannot separate these two components, it is important to investigate the difference between the production off free and bound protons. In Fig. 4 we compare the four-momentum transfer distribution for both sets where we assume a free proton in set II for the calculation. The small difference can be associated with the neglect of the Fermi motion. The effective K^+K^- mass distributions are compared in Fig. 5 for a four-momentum transfer $0.01 \leqslant |t| \leqslant 0.2\ \mathrm{GeV}^2$. The spectra are within the errors identical. As it will be shown in the next section, we also observe agreement for the polarization independent moments of K^+K^- decay angular distributions. Thus the results of both experiments will be used in our analysis.

3. *Moments of the angular distribution*

The K^+K^- angular distribution for a given energy can generally be written in the form:

$$W(m_{KK}, t, \theta, \varphi) = \sum_{L, M} \overline{t_M^L}(m_{KK}, t) \cdot \mathrm{Re}\ Y_M^L(\cos\theta, \varphi), \tag{2}$$

where m_{KK} is the effective mass of the K^+K^- system, Y_M^L are the spherical harmonic functions, θ, φ are the decay angles of the K^- in the K^+K^- rest system, $\overline{t_M^L}\,(m_{KK}, t)$ are the moments of the angular distribution normalized in such a way that $\overline{t_0^0} = 1/\sqrt{4\pi}$.

In this paper we interpret the unnormalized moments $t_M^L \overset{\mathrm{df}}{=} \dfrac{d^2\sigma}{dt dm_{KK}}\,\overline{t_M^L}$. The $L = 4$, $M = 0, 1, 2$ moments can be expressed in terms of the P, D and F flip and nonflip amplitudes (for the definitions of partial wave amplitudes, see Ref. [4]):

$$t_0^4 = 0.86|D_0|^2 - 0.57(|D_U|^2 + |D_N|^2) + 0.60|F_0|^2 + 0.09(|F_U|^2 + |F_N|^2) + \{(PF^*)\text{-terms}\}, \tag{3}$$

$$t_1^4 = 1.11(D_0D_U^*) + 0.50(F_0F_U^*) + \{(PF^*)\text{-terms}\}, \tag{4}$$

$$t_2^4 = 0.45(|D_U|^2 - |D_N|^2) + 0.29(|F_U|^2 - |F_N|^2) + \{(PF^*)\text{-terms}\} \tag{5}$$

with

$$|D_0|^2 = |D_0^f|^2 + |D_0^n|^2, \quad (D_0D_U^*) = \mathrm{Re}\,(D_0^f D_U^{f*}),\ \text{etc.},$$

where f and n indicate nucleon spin flip and spin nonflip. D_0 is the helicity $m = 0$ partial wave amplitude (unnatural spin-parity exchange) and D_N (D_U) is the helicity $m = 1$ amplitude corresponding to natural (unnatural) spin-parity exchange, respectively.

The mass spectrum, as shown in Fig. 5, is dominated by a broad peak between 1200 and 1500 MeV. The mass dependence of the unnormalized t_M^4 ($M = 0, 1, 2$) in this range is shown in Fig. 6. The higher M-moments are, as the $M = 2$, compatible with zero.

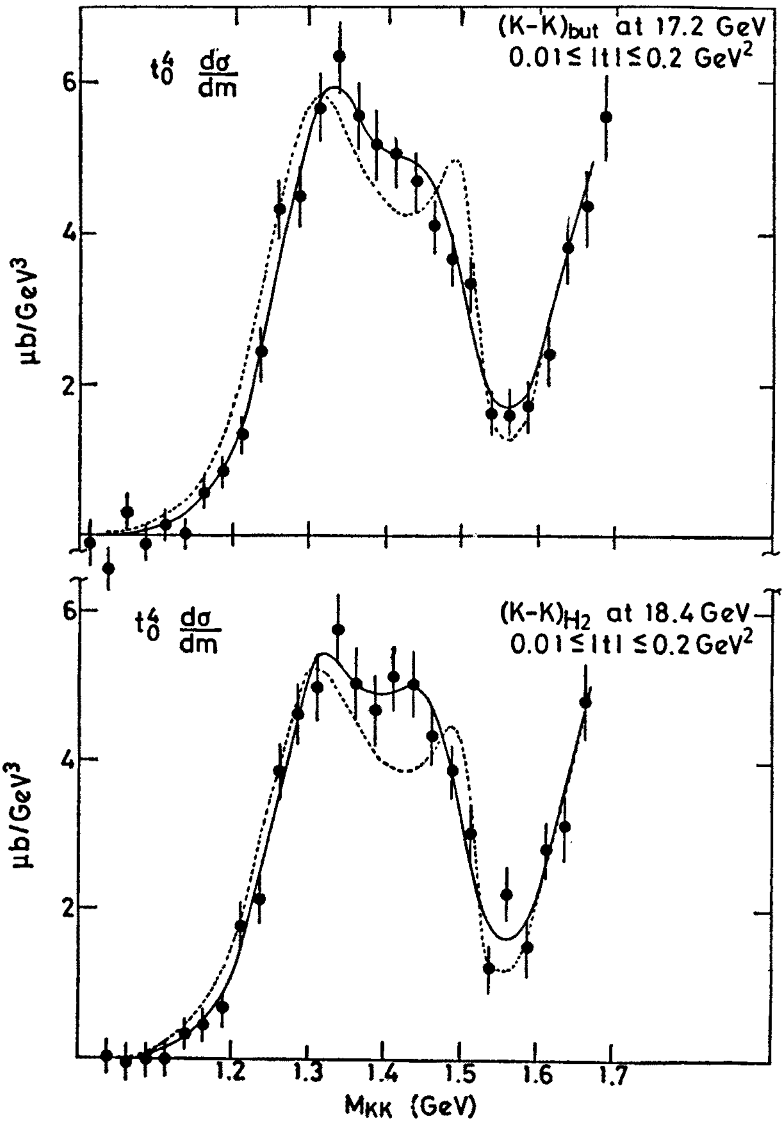

a

The $|t|$ range for Figs. 5 and 6 is chosen to be between 0.01 and 0.20 GeV^2. The lower limit was taken to avoid any influence from $|t_{min}|$ variation as a function of mass. The upper limit was set at $|t| = 0.2$ GeV^2 as the $|t|$ dependence of the normalized $\overline{t_M^4}$ moments ($M = 0, 1, 2$) vary only weakly below this value as shown in Fig. 7.

It is seen immediately that the t_0^4 moment shows the features of the above mentioned peak in the mass distribution, i.e. a peak at ~ 1350 MeV, a small enhancement, or at least a shoulder, around ~ 1450 MeV and a dip around ~ 1550 MeV. Using the amount of

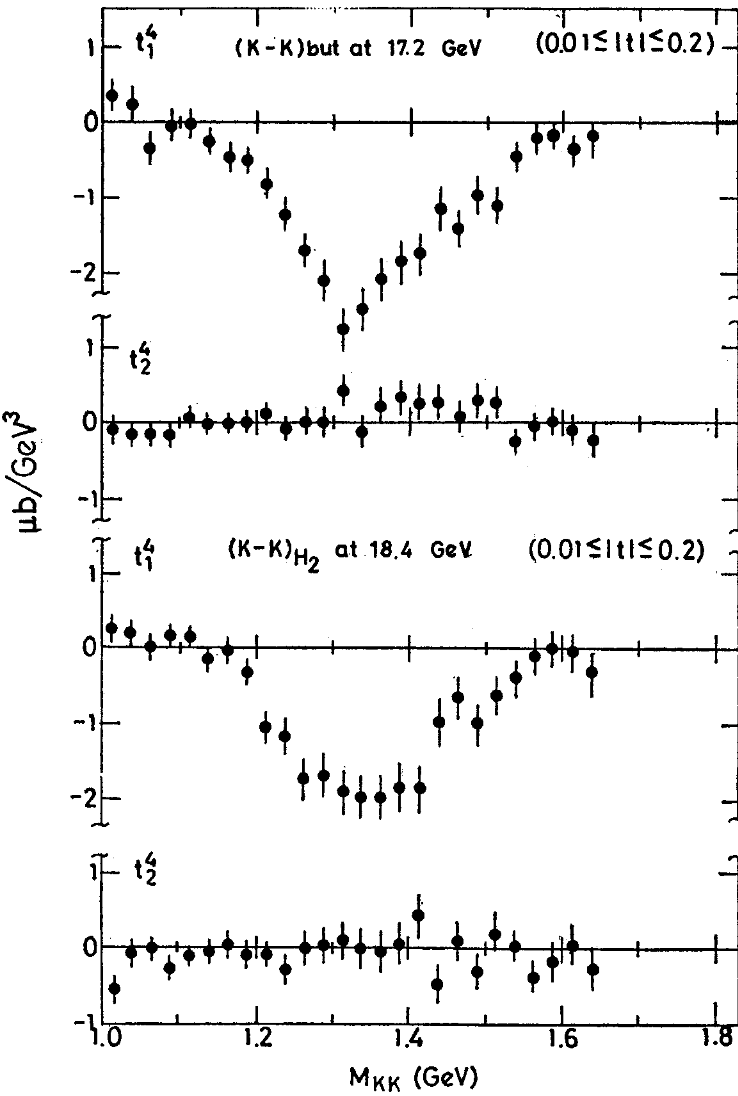

b

Fig. 6. Mass dependence of the unnormalized moments t_0^4, t_1^4 and t_2^4 for $0.01 < |t| < 0.2\ \mathrm{GeV}^2$ (butanol and hydrogen)

t_0^4 we estimate that the spin 2 states contribute at least to 70% of the mass spectrum ($|t| < 0.2\ \mathrm{GeV}^2$). This D-wave dominance has been observed in three partial wave studies, namely:

(*i*) the $K_S^0K_S^0$ results of the CERN-ETH Collaboration [5] at 8.9 GeV and of the Notre Dame Group at 6 and 7 GeV [6];
(*ii*) an analysis of the K^+K^- system at 6 GeV performed by the Argonne Group [7];
(*iii*) a model-independent analysis of our data performed in Ref. [1].

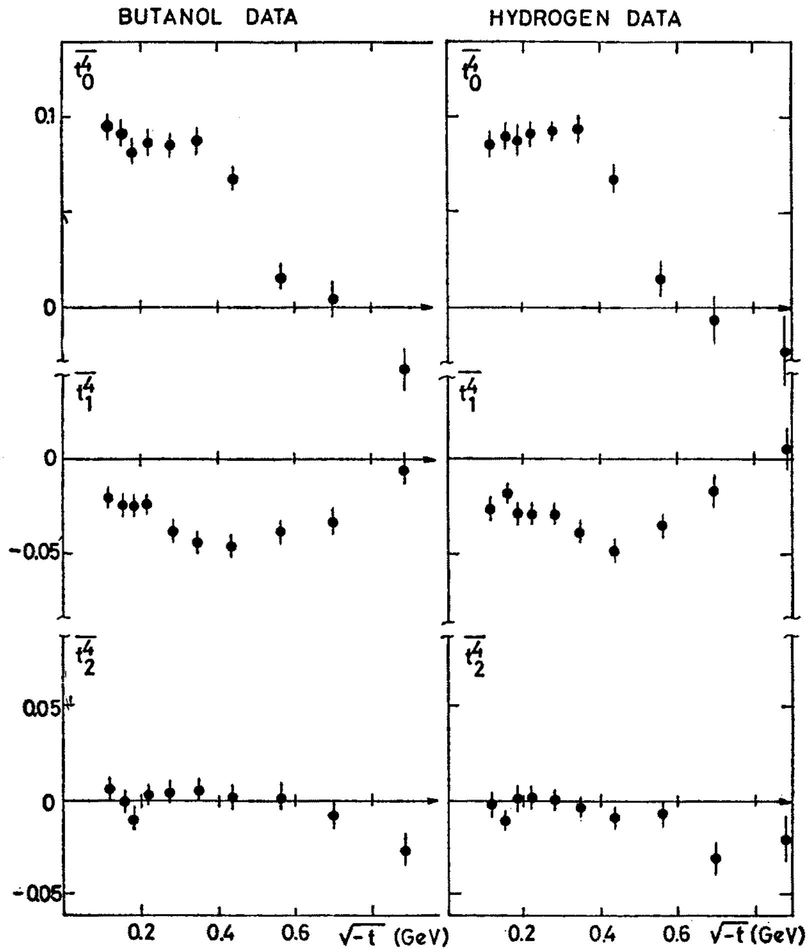

Fig. 7. t-dependence of the normalized moments: $\overline{t_0^4}$, $\overline{t_1^4}$, and $\overline{t_2^4}$ in the $1.00 < m_{KK} < 1.55$ GeV mass region for butanol and hydrogen data

Assuming that the F-wave can be neglected in the mass range under consideration, the vanishing of the t_2^4 moment indicates that $|D_U|^2 = |D_N|^2$. With the same assumption, a comparison of the t_0^4 and t_1^4 moments shows that $|D_U|^2 \ll |D_0|^2$. Therefore also $|D_N|^2 \ll |D_0|^2$.

It is instructive to compare our K^+K^- results with the $\pi^+\pi^-$ ones at 17.2 GeV from Ref. [8]. It is seen in Fig. 8 that for the $\pi^+\pi^-$ data the peak in the mass spectrum and t_0^4 moment are exactly at the position of the f(1270) resonance and the dip is around

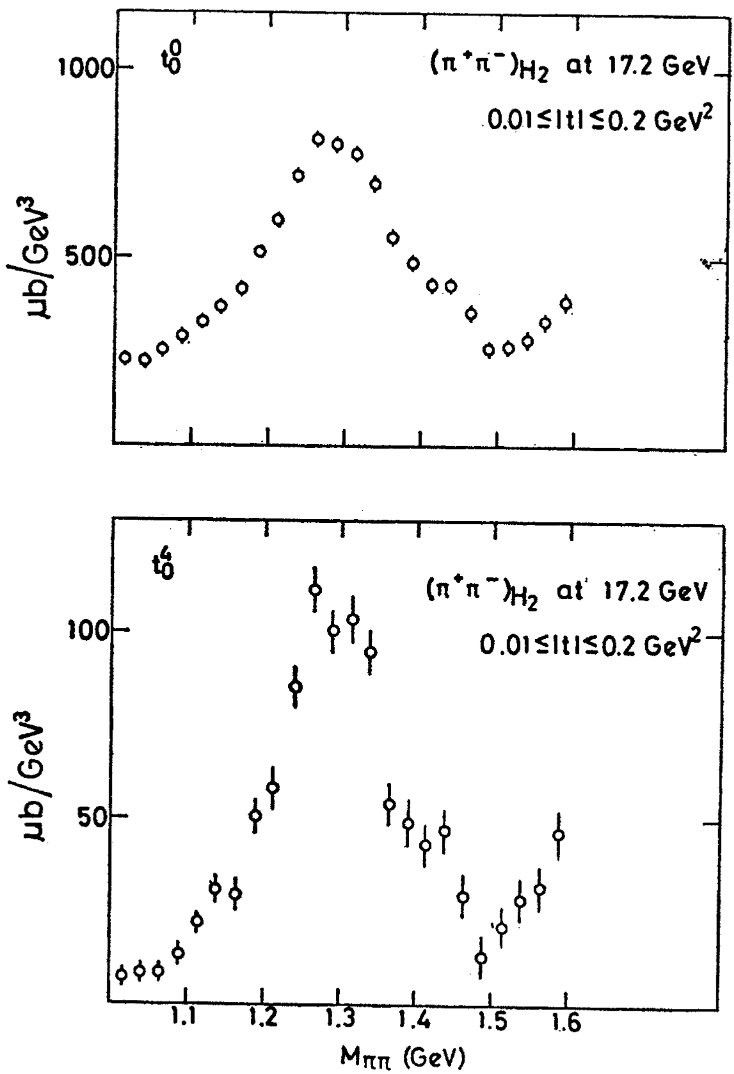

Fig. 8. $\pi^+\pi^-$ invariant mass spectrum and mass dependence of the t_0^4 moment for $0.01 < |t| < 0.2$ GeV^2 for the hydrogen target data

$\sim$1480 MeV contrary to the K^+K^- data. One of the reasons for this difference can be a small $A_2(1310)$ and a large f′(1515) signal in the K^+K^- data. The coupling of these resonances to the $\pi\pi$ channel is forbidden and suppressed, respectively.

4. Fits to the D-wave

In this section, a superposition of interfering D-wave resonances $f(1270)+A_2(1310)+f'(1515)$ is fitted to the t_0^4 moment. It is assumed that the t_0^4 moment contains only $|D^2|$ and $|F^2|$ terms, where the F-wave is described by the g(1690) resonance. More precisely, it is assumed that:

$$|D_U|^2 \sim |D_0|^2, \quad |D_N|^2 \sim |D_0|^2, \quad \mathrm{Re}\,(PF^*) \simeq 0.$$

The results of a model-independent partial wave analysis of our data [1] show that these relations are reasonably satisfied.

For resonant K^+K^- production we factorize the $\pi^-p \to K^+K^-n$ amplitude into a term C_i describing the production of the i-th resonance and a term describing the decay into the K^+K^- channel which contains the mass dependence, i.e. the Breit-Wigner decay amplitude $B_i(m_{KK})$. Thus the general formula for our fit is

$$t_0^4 = \frac{m^2}{q_\pi}\{|C_f K_f^f \cdot B_f(m) + C_{f'} K_{f'}^f e^{i\phi_{f'}^f} \cdot B_{f'}(m) + C_{A_2} K_{A_2}^f e^{i\phi^f_{A2}} \cdot B_{A_2}(m)|^2$$

$$+|C_f K_f^n \cdot B_f(m) + C_{f'} K_{f'}^n e^{i\phi_n^{f'}} \cdot B'_{f'}(m) + C_{A_2} K_{A_2}^n e^{i\phi^n_{A2}} \cdot B_{A_2}(m)|^2 + |C_g \cdot B_g(m)|^2\} \qquad (6)$$

C_i — coefficient including normalization factor and elasticities, $\phi_{f'}^f$, $\phi_{A_2}^f$, $\phi_{f'}^n$, $\phi_{A_2}^n$ — production phases of the f′ and A_2 resonances relative to the f-meson, where f and n indicate nucleon spin flip and nonflip, m — effective mass of K^+K^- system, $q_\pi = \sqrt{m^2/4 - m_\pi^2}$, $K_i^f = 1/\sqrt{1+\xi_i^2}$, $K_i^n = \xi_i/\sqrt{1+\xi_i^2}$, where ξ_i is the nonflip/flip ratio of the i-th resonance. Explicitly the general formula contains the terms

$$|C_i B_i|^2 + |C_j B_j|^2 + |C_k B_k|^2$$

$$+2C_i C_j\,\mathrm{Re}\,(B_i B_j^*) \cdot [K_i^f K_j^f \cos\phi_{ij}^f + K_i^n K_j^n \cos\phi_{ij}^n]$$

$$+\ \dots\ 2C_i C_j\,\mathrm{Im}\,(B_i B_j^*) \cdot [K_i^f K_j^f \sin\phi_{ij}^f + K_i^n K_j^n \sin\phi_{ij}^n] + \dots$$

where the indices i, j, k stand for the f, f' and A_2 resonances.

We used the Breit-Wigner formula of the following form:

$$B(m) = \frac{m_R\sqrt{\Gamma_{\pi X}\cdot\Gamma_{KK}}}{m_R^2 - m^2 - i m_R \Gamma_{tot}},$$

where

$$\Gamma_{\pi X} = X_{\pi X}\cdot\Gamma\cdot\left(\frac{q_{\pi X}}{q_{\pi X}^R}\right)^5\cdot\frac{D_2(q_{\pi X}^R r)}{D_2(q_{\pi X} r)},$$

$$\Gamma_{KK} = X_{KK}\cdot\Gamma\cdot\left(\frac{q_{KK}}{q_{KK}^R}\right)^5\cdot\frac{D_2(q_{KK}^R r)}{D_2(q_{KK} r)},$$

$q_{KK} = \sqrt{m^2/4 - m_K^2}$; $q_{KK}^R = q_{KK}(m = m_R)$; $q_{\pi X}$ — is the value of the decay channel momentum $m \to m_\pi + m_X$, where $m_X = m_\pi$ for the f, f′, g and $m_X = m_\varrho$ for A_2; $q_{\pi X}^R = q_{\pi X}(m = m_R)$, $X_{\pi X}(X_{KK})$ — elasticity of the resonance R.

$$\Gamma_{tot} = \Gamma\left(\frac{q}{q^R}\right)^5\frac{D_2(q^R r)}{D_2(q r)},$$

where q is the decay momentum in the main decay channel of the resonance, namely: $q = q_{\pi\pi}$ for f and g, $q = q_{KK}$ for f′ and $q = q_{\varrho\pi}$ for A_2.

For spin 2 resonances we take the barrier penetration factor to be $D_2(qr) = (qr)^4 + 3(qr)^2 + 9$ and the radius to be 1 fm. Generally, the parameters to be determined by the data were the coefficients C multiplied by the product of elasticities $\sqrt{X_{in} \cdot X_{out}}$, the total

TABLE II

		$0.01 \leq \lvert t \rvert \leq 0.20\ GeV^2$				
		K^+K^-n H_2	K^+K^-n H_2 + but	K^+K^-n H_2	K^+K^-n H_2 + but	K^+K^-n K^+K^-p Argonne
		Fit 1	Fit 1′	Fit 2	Fit 2′	Fit 3
1	C_f	$1.16^{+0.14}_{-0.14}$	$1.20^{+0.09}_{-0.09}$	$1.20^{+0.12}_{-0.12}$	$1.25^{+0.08}_{-0.08}$	$5.99^{+0.13}_{-0.12}$
2	m_f	1275	1275	1275	1275	1275
3	Γ_f	180	180	180	180	180
4	ξ_f	0	0	0.25	0.25	0.25
5	$C_{f'}$	$1.20^{+0.31}_{-0.29}$	$1.18^{+0.21}_{-0.20}$	$1.19^{+0.28}_{-0.26}$	$1.17^{+0.18}_{-0.17}$	$2.50^{+0.61}_{-0.43}$
6	$m_{f'}$	1499^{+9}_{-10}	1508^{+7}_{-8}	1497^{+8}_{-9}	1503^{+6}_{-7}	1496^{+9}_{-8}
7	$\Gamma_{f'}$	140^{+22}_{-20}	146^{+18}_{-17}	137^{+23}_{-21}	144^{+19}_{-17}	69^{+22}_{-16}
8	$\phi^{f}_{f'}$	$191° \pm 20°$	$192°^{+11°}_{-13°}$	$186°^{+15°}_{-21°}$	$187°^{+10°}_{-12°}$	$146° \pm 23°$
9	$\phi^{n}_{f'}$	—	—	$186°^{+15°}_{-21°}$	$187°^{+10°}_{-12°}$	$146° \pm 23°$
10	$\xi_{f'}$	0	0	0.25	0.25	0.25
11	C_{A_2}	$0.30^{+0.15}_{-0.15}$	$0.40^{+0.11}_{-0.11}$	$0.53^{+0.22}_{-0.22}$	$0.65^{+0.16}_{-0.15}$	$1.70^{+0.46}_{-0.49}$
12	m_{A_2}	1310	1310	1310	1310	1310
13	Γ_{A_2}	100	100	100	100	100
14	$\phi^{f}_{A_2}$	$355° \pm 45°$	$341° \pm 23°$	290°	290°	290°
15	$\phi^{n}_{A_2}$	—	—	$1° \pm 84°$	$338° \pm 48°$	$388°^{+36°}_{-19°}$
16	ξ_{A_2}	0	0	4.0	4.0	4.0
17	C_g	$1.28^{+0.04}_{-0.04}$	$1.28^{+0.03}_{-0.03}$	$1.27^{+0.04}_{-0.04}$	$1.26^{+0.03}_{-0.03}$	$3.57^{+1.21}_{-1.80}$
18	m_g	1690	1690	1690	1690	1690
19	Γ_g	180	180	180	180	180
χ^2/ND		20.8/19	56.2/46	21.4/19	58.2/46	45.0/38

widths Γ, the masses m_R, and the relative phases ϕ^f and ϕ^n. We tried the fits for the various values of the parameter ξ.

The above formula has been fitted to the t_0^4 moment in 25 MeV bins from 1025 MeV to 1700 MeV in a $|t|$ bin from 0.01 GeV^2 to 0.2 GeV^2.

The results of our fits are shown in Table II. In these fits the positions and widths of f(1270), A_2(1310), and g(1690) have been fixed at their Particle Data Group [9] values (in Table II the fixed parameters appear without errors).

5. Discussion of results and comparison with other experiments

We do not have enough data to allow all resonance masses, widths, relative phases and ξ to be determined by the fit. While it is reasonable to fix the mass and width of the f and A_2 to their table value we have left the mass and width of the f′ to be free. Further we had to fix the nonflip/flip ratio ξ. In the first series of fits 1(1′) we varied ξ only around zero corresponding to the full coherence. This is well justified for the f and the f′ production (OPE mechanism [1]) while a good justification for $\xi_{A_2} = 0$ (dominance of B exchange) is missing. Partly this problem is related to the fact that we do not have a precise independent measurement for the $A_2 \rightarrow K\bar{K}$ as we have for the $f \rightarrow \pi\pi$. Actually there are indications that the A_2 is produced dominantly by Z_0-exchange giving rise to a high value of ξ_{A_2}. Therefore in second group of fits 2(2′) we used a value of $\xi_f = \xi_{f'} = 0.25$ and $\xi_{A_2} = 4$. The value of $\xi_{A_2} = 4$ has been extracted from the Argonne data [7] at 6 GeV by repeated fits varying ξ_{A_2} in small steps. We further assume that ξ_{A_2} does not change from 6 to 18 GeV. In summary we obtain acceptable χ^2/ND for both groups of fits but always requiring a nonnegligible amount of A_2 production around 8%.

Our fits require an f′ of about 140 MeV width and a mass very close to 1500 MeV. In particular the obtained width is completely inconsistent with the current measured values. Both fits 1(1′) and 2(2′) require substantial amount of f′. For the relative production phases we obtained values around 0° for the A_2 and around 180° for the f′. If the f′ is produced by the same production mechanisms as the f one expects relative phase 0° or 180°.

We tried to fix also the f′ to the table values of $m_{f'} = 1515$ MeV and $\Gamma_{f'} = 65$ MeV. We obtain a $\chi^2/\mathrm{ND} = 57/22$ for the hydrogen data and $\chi^2/\mathrm{ND} = 66/22$ for the butanol data. Therefore either the f′ is wider and at lower mass or another description of the data is needed. Before considering this possibility we would like to discuss and compare data of other experiments at lower energies.

Pawlicki et al. [7] have analyzed the t_0^4 moments of the Argonne data for the reactions $\pi^- p \rightarrow K^+K^- n$ and $\pi^+ n \rightarrow K^+K^- p$ at 6 GeV as a function of m_{KK}. The t_0^4 moments were interpreted in terms of interference between f, f′, and A_2 resonance production. The sum and difference of these moments may be symbolically expressed in terms of these resonance production amplitudes [10].

$$\Sigma(t_0^4) \sim |f|^2 + |f'|^2 + 2\,\mathrm{Re}\,(ff'^*) + |A_2|^2$$

$$\Delta(t_0^4) \sim \mathrm{Re}\,(fA_2^*) + \mathrm{Re}\,(f'A_2^*).$$

The $\Sigma(t_0^4)$ data show clear evidence of an f-f′ interference effect and allow a determination of the $f' \to \pi\pi$ branching ratio. On the other hand, the data for $\Delta(t_0^4)$ show little evidence for f-A_2 interference, but do show structure (at least for band $0.08 < |t| < 0.2\ \mathrm{GeV}^2$) which may be attributed to f′-A_2 interference.

We have applied our formula (6), as described above, to the Argonne data [7] at 6 GeV for $|t| < 0.2\ \mathrm{GeV}^2$ and simultaneously performed a fit to the $\pi^- p \to K^+K^- n$ and $\pi^+ n \to K^+K^- p$ reactions. In this fit we have assumed the same ratio of nonflip/flip amplitude for f and f′ resonances, namely $\xi_f = \xi_{f'} = 0.25$. From our partial wave analysis of $\pi^- p$

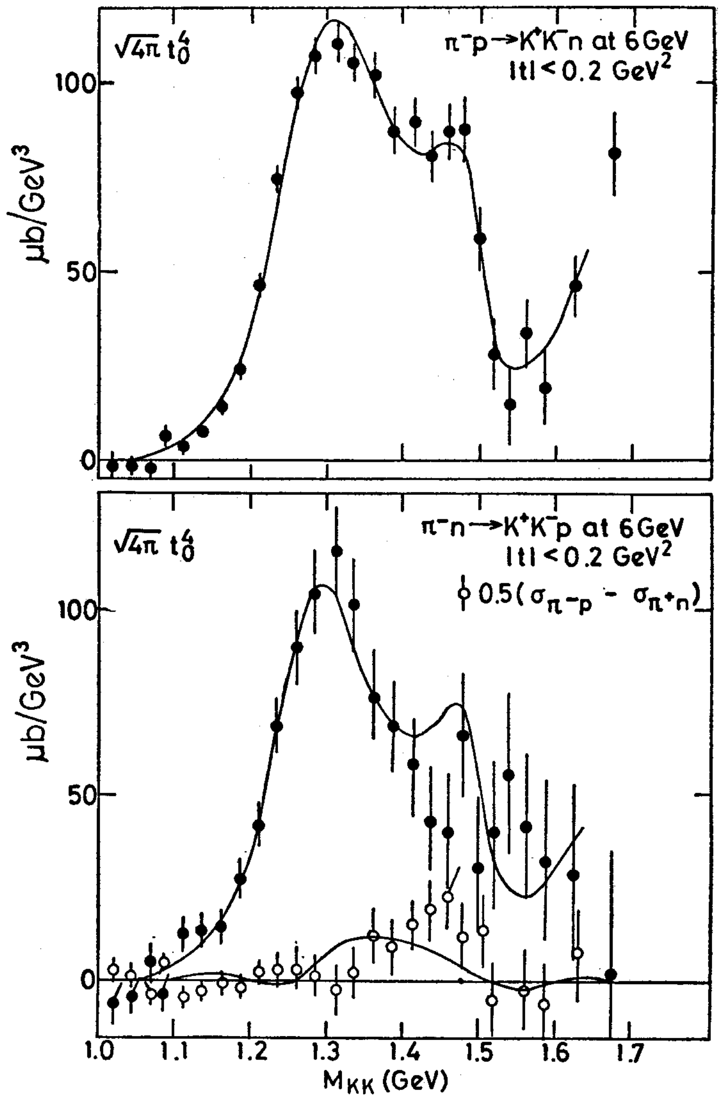

Fig. 9. Mass dependence of the $\sqrt{4\pi}\ t_0^4$ moments for $|t| < 0.2\ \mathrm{GeV}^2$ from the Argonne data at 6 GeV on $\pi^- p \to K^+K^- n$ and $\pi^+ n \to K^+K^- p$

$\to \pi^+\pi^-n$ data [8] we know that this ratio is $R_f > 0.16$ for the f(1217). The results of our fit to the Argonne data are listed in Table II (Fit 3) and are shown in Fig. 9. The results of our fit to the Argonne data can be summarized as follows:

1. It can be seen that our results do not violate the Schwarz-type inequalities $|f'| \cdot |A_2| \geqslant \mathrm{Re}(f'A_2^*)$ as in the original ANL analysis [7] of the t_0^4 moments.

2. We are able to produce a sizable f′-A_2 interference effect and satisfactorily fit the data only with a nonflip A_2 amplitude (Z-exchange) and small nonflip amplitude for the f and f′ (A_1-exchange).

3. The contribution of f′ is much larger than that obtained in the ANL analysis. Our fit yields the relative intensity ratio $C_{f'}^2/C_f^2 \simeq 0.17$.

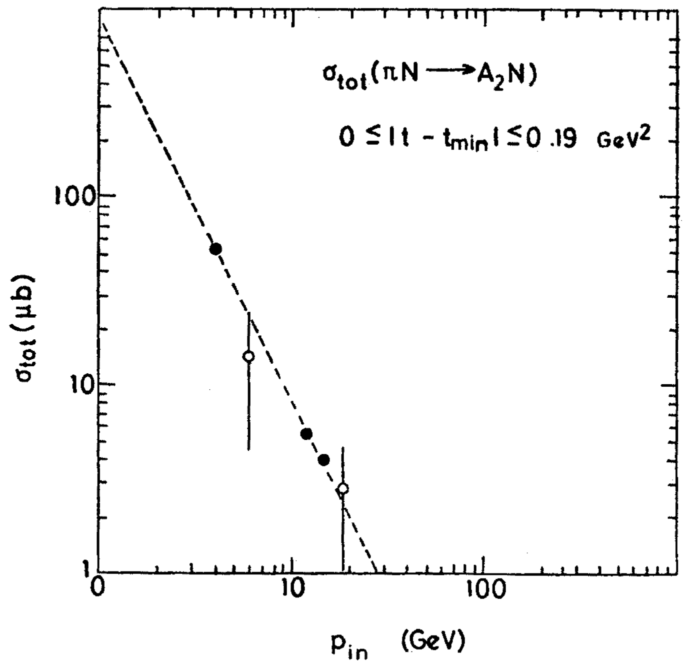

Fig. 10. Total cross-section $\varrho_{00}\sigma(\pi N \to A_2N)$ vs incident beam momentum for A_2 production for $|t| < 0.2\ \mathrm{GeV}^2$

4. From results of our fit to the ANL data at 6 GeV, the estimated value of the total cross section $\sigma_{00} \cdot \varrho(\pi N \to A_2)$ for A_2 production, fairly agrees (if one assumes a p_{in}^2 dependence) with the data on the $\pi N \to A_2N$ reaction [11, 12] at 4, 12, and 15 GeV as is shown in Fig. 10.

5. The values of $m_{f'}$ and $\Gamma_{f'}$ are compatible with those obtained in the original ANL analysis [7] of the t_0^4 moments.

In summary the low energy data can be reasonably described by a narrow f′ and very small amount of A_2, while our data at 17 and 18 GeV always require a wide f′ and fits improve also by adding a small amount of A_2. From our fits 2(2′) we extract an A_2 total cross-section of 2.0 μb as shown in Fig. 10 (we used BR($A_2 \to K\bar{K}$) = 4.7%). As we need the A_2 contribution one is able to predict the shape for $K_S^0K_S^0$ data from fits 1(1′) and 2(2′). For full coherence assumption, fit 1(1′), we expect a markedly different shape for the t_0^4 moment in the $K_S^0K_S^0$ data while for the fit 2(2′) very similar spectra are expected. As there are no $K_S^0K_S^0$ data around 18 GeV a direct comparison cannot be made, but the low energy data at 6, 7 and 8.9 GeV are more in agreement with predictions of fit 2(2′).

5.1. Parameters of the f′ resonance

Our fits yield $m_{f'} = (1503 \pm 7)$ MeV, $\Gamma_{f'} = (144 \pm 18)$ MeV and $\phi_{f'f} = (187 \pm 11)^0$. The value $\Gamma_{f'}$ contradicts the results on the reactions

$$K^-p \to K^+K^-\Lambda(\Sigma^0), \quad K^-p \to K_S{}^0K_S{}^0\Lambda(\Sigma^0), \tag{7}$$

TABLE III

	Source	$m_{f'}$ (MeV)	$\Gamma_{f'}$ (MeV)	$f' \to \pi\pi$
1	Particle Data Group [9]	1516 ± 12	67 ± 10	seen
2	Brandenburg et al. [14] $\pi^-p \to K^+K^-\Lambda(\Sigma^0)$ at 13 GeV	1527 ± 5	61 ± 8	$\frac{f' \to \pi^+\pi^-}{f' \to \bar{K}K} \leqslant 6\%$ (90% CL)
3	Barreiro et al. [15] $K^-p \to K_S^0K_S^0$ at 4.2 GeV	1522 ± 6	62^{+19}_{-14}	$\frac{f' \to \pi^+\pi^-}{f' \to \bar{K}K} \leqslant 4.3\%$ (95% CL)
	$K^-p \to K^+K^-$ at 4.2 GeV	1520 ± 13	83 ± 23	
4	Evangelista et al. [17] $K^-p \to K^+K^-\Lambda(\Sigma^0)$ at 10 GeV	1528 ± 7	72 ± 25	
5	Beusch et al. [16] $\pi^-p \to K_S^0K_S^0$ at 8.9 GeV	—	—	$\frac{f' \to \pi\pi}{f' \to \text{all}} \leqslant 1\%$
6	Pawlicki et al. [7] $\pi^-p \to K^+K^-n$ at 6 GeV	1506 ± 5	66 ± 10	$\frac{f' \to \pi\pi}{f' \to \text{all}} = (1.2\ 0.4)\%$

which yield the f′ mass about 1520 MeV and the width around 65 MeV (see Table III). As already remarked by the Argonne group [7], these results can be affected by neglecting the interference between the f′ and small contributions of the f and A_2 production and also by the procedure of background subtraction (the resonance curve has been fitted directly to the mass spectrum).

5.2. The $f \to K\bar{K}$ branching ratio

The branching ratio of the f(1270) resonance into $\bar{K}K$ has been determined from its contributions, C_f, obtained in the fits to the K^+K^- data at 18.4 GeV and the $\pi^+\pi^-$ data at 17.2 GeV. Both sets of data were taken with the same apparatus and the same mass and $|t|$ range have been used for fits. In the fit to the t_0^4 moment of the $\pi^+\pi^-$ data, the terms involving the $A_2(1310)$ resonance have been neglected.

The branching ratio obtained from our fits is

$$\frac{f \to K^+K^-}{f \to \pi^+\pi^-} = \left(\frac{C_f^{(K)}}{C_f^{(\pi)}}\right)^2 = \left(\frac{1.20\pm0.12}{6.98\pm0.16}\right)^2 = 0.0295\pm0.0061.$$

After corrections for difference in beam momentum $(18.4/17.2)^2 = 1.14$, the isospin relations $K^+K^-/\bar{K}K = 1/2$ and $\pi^+\pi^-/\pi\pi = 2/3$ and taking f(1270) elasticity to be 0.803 from Ref. [9], the final branching ratio is

$$\frac{f \to \bar{K}K}{f \to \text{all}} = (3.60\pm0.74)\%.$$

In the calculation of errors the uncertainty of normalization between these two experiments (~ 5% for each) has been neglected. Our branching ratio is consistent with the Particle Data Group [9] average of (3.1±0.4)%.

5.3. The $f' \to \pi\pi$ branching ratio

Our fits show a strong f-f′ interference effect. The relative production phase $\phi_{f'f} = (187\pm11)^\circ$ is consistent with the OPE production mechanism which allows either 0° or 180°. Therefore we assume that both the f(1270) and f′(1515) are produced mainly (the contribution of flip amplitude to the cross-section is $1/(1+\xi^2_{f(f')}) \simeq 0.96$) via OPE in π-induced reactions. Using this assumption, we can determine the $f' \to \pi\pi/f' \to \text{all}$ branching ratio in the following way:

From our fit (Fit 2 in Table II) to reaction (1) we have

$$\frac{(f' \to \pi^+\pi^-/f' \to \text{all})\cdot(f' \to K^+K^-/f' \to \text{all})}{(f \to \pi^+\pi^-/f \to \text{all})\cdot(f \to K^+K^-/f \to \text{all})} = \frac{C_{f'}^2}{C_f^2} = 0.88\pm0.29.$$

Now using $f \to \pi\pi/f \to \text{all} = 80.3\%$ and $f \to \bar{K}K/f \to \text{all} = 3.1\%$ from the last PDG edition [9] yields:

$$\frac{f' \to \pi\pi}{f' \to \text{all}}\cdot\frac{f' \to \bar{K}K}{f' \to \text{all}} = (2.2\pm0.7)\%.$$

Taking the SU_3 prediction [13] for the branching ratio of $f' \to \bar{K}K/f' \to \text{all} = 70\%$, we obtain

$$\frac{f' \to \pi\pi}{f' \to \text{all}} = (3.0\pm1.0)\%.$$

This value is consistent with those of Refs. [14, 15] but higher than the (1.2±0.4)% quoted by the Argonne group and 1% given by the CERN-ETH Collaboration [16].

6. A possible new 2^+ meson at 1430 MeV

As we have already stated our data cannot be fitted by the table parameters of the f′(1515). The main discrepancy is in the mass region (1400–1450) MeV. Here, contrary to the fitted curve (dashed line in Fig. 6a), a small enhancement is observed. In order to obtain a reasonable description of the t_0^4 moment with the table values of the f′(1515) one has to add incoherently a fourth D-wave resonance to the coherent sum of the f(1270), A_2(1310), and f′(1515) already included in our fits (because of limited statistics we have assumed the simplest version). In this case, the fit yields for this new object m = (1422±9)

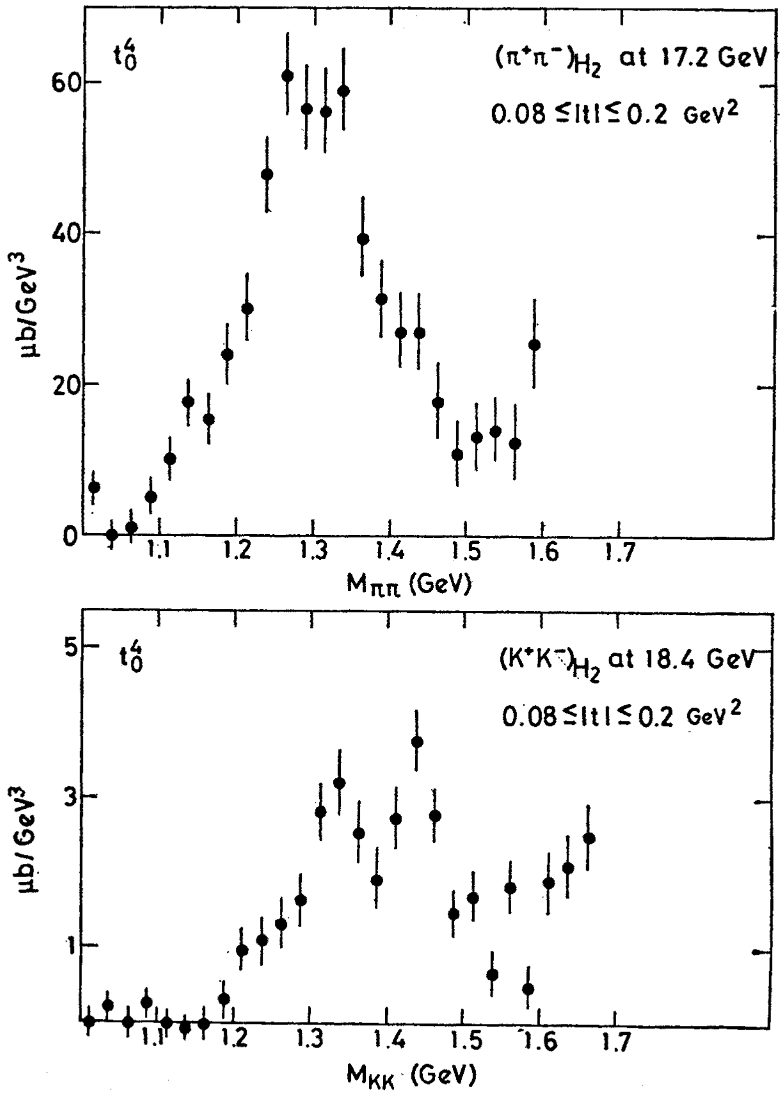

Fig. 11. Mass dependence of the t_0^4 moments in the interval $0.08 < |t| < 0.2$ GeV² for the $\pi^+\pi^-$ and K^+K^- data

MeV and Γ = (80±42) MeV with a reasonable χ^2/ND = 21/18. The existence of such an object called X(1410–1440) has been indicated in the old $\varrho^0\varrho^0$ and $\overline{K}K$ results — see the Particle Data Group listings. As mentioned in Section 5, the Notre Dame group [6] has attributed this enhancement to the f(1275)+f′(1515) interference, but this explanation does not work for our results.

It is interesting to note that this enhancement becomes relatively stronger with increasing four-momentum transfer. In Fig. 11 the t_0^4 moment is shown for the t interval (0.08–-0.20) GeV^2. There is a clear peak at ~ 1435 MeV in the K$^+$K$^-$ data. At still higher values

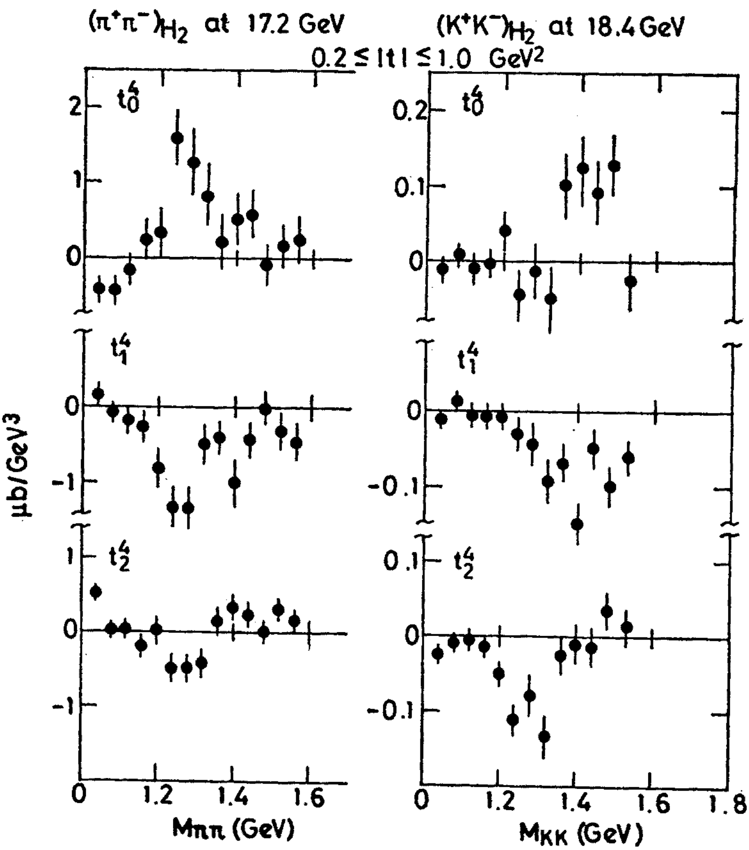

Fig. 12. Mass dependence of the unnormalized moments: t_0^4, t_1^4 and t_2^4 for $0.2 < |t| < 1.0$ GeV^2 for $\pi^+\pi^-$ and K$^+$K$^-$ hydrogen target data

of the four-momentum transfer it is only this peak which is seen, the first one at ~ 1330 MeV having completely disappeared as shown in Fig. 12. Unfortunately, low statistics does not allow us to make a detailed fit in this region.

One should bear in mind that a possible new D-wave resonance does not fit easily into a quark scheme, the $J^{PC} = 2^{++}$ nonet being already full. Also its quark structure is not clear. If it is constructed of non-strange quarks like the f(1275) it should be seen in the reaction $\pi^-p \rightarrow \pi^+\pi^-n$. If it is built of strange quarks like the f′(1515) it should be observed in the reaction $K^-p \rightarrow K^+K^-\Lambda(\Sigma)$. Therefore this hypothetical new object finds no easy explanation; one could even speculate about its glueball nature. The dual string model of Freund and Nambu [18] and Robson [19] predicts some particles in the pomeron sector. Assuming the linear trajectory of the slope equal to 0.5 and intercept equal to 1, one expects the first particle with $J^{PC} = 2^{++}$ at a mass of $\sqrt{2}$ GeV.

Let us remember that this object is not needed if the f′(1515) is in fact at ~ 1500 MeV and wider than 100 MeV. In any case further studies of the $\overline{K}K$ system with high statistics and good acceptance are clearly needed.

REFERENCES

[1] H. Becker et al., *Nucl. Phys.* **B174**, 16 (1980).
[2] W. Blum et al., *Phys. Lett.* **57B**, 403 (1975); G. Hentschel, Thesis, Max Planck Institute, Munich, April 1976.
[3] H. Becker et al., *Nucl. Phys.* **B150**, 301 (1979); J. De Groot, Thesis, University of Amsterdam, April 1978.
[4] G. Lutz, K. Rybicki, MPI-PAE/Exp. E1.75, October 1978.
[5] W. Wetzel et al., *Nucl. Phys.* **B115**, 208 (1976).
[6] V. A. Polychronakos et al., *Phys. Rev.* **D19**, 1317 (1979).
[7] A. J. Pawlicki et al., *Phys. Rev.* **D15**, 3196 (1977).
[8] G. Grayer et al., *Nucl. Phys.* **B75**, 189 (1974); H. Becker et al., *Nucl. Phys.* **B151**, 46 (1979).
[9] Review of Particle Properties, *Rev. Mod. Phys.* **52**, 51 (1980).
[10] H. J. Lipkin, *Phys. Rev.* **176**, 1709 (1968).
[11] M. J. Corden et al., *Nucl. Phys.* **B138**, 235 (1978).
[12] M. J. Emms et al., *Phys. Lett.* **58B**, 117 (1975).
[13] N. P. Samios, M. Goldberg, B. T. Meadows, *Rev. Mod. Phys.* **46**, 49 (1974).
[14] G. W. Brandenburg et al., *Nucl. Phys.* **B104**, 413 (1976).
[15] F. Barreiro et al., *Nucl. Phys.* **B121**, 234 (1977).
[16] W. Beusch et al., *Phys. Lett.* **60B**, 101 (1975).
[17] C. Evangelista et al., *Nucl. Phys.* **B127**, 384 (1977).
[18] P. G. D. Freund, Y. Nambu, *Phys. Rev. Lett.* **B34**, 1645 (1975).
[19] D. Robson, *Nucl. Phys.* **B130**, 328 (1977).